

Experimental cyclic response of ductile partially-encased composite members

C. Málaga-Chuquitaype, A.Y. Elghazouli & X. Ban

Imperial College London, UK



SUMMARY:

This paper deals with the experimental behaviour of partially-encased composite members subjected to combined bending and axial loading. A detailed account of the results of seven cyclic bending tests with axial compression ranging from 10% to 20% of the axial plastic capacity is presented. A description of the experimental arrangement and material properties is given, and the main experimental results and salient behavioural observations are discussed. The response of conventional partially-encased sections as well as details incorporating two forms of local buckling delaying configurations is investigated and discussed. The discussion focuses on issues related to ductility considerations and failure modes under severe cyclic loading. Response parameters related to energy dissipation and cumulative displacements at failure are highlighted.

Keywords: Ductility, partially-encased members, cyclic load, energy dissipation

1. INTRODUCTION

Composite steel/concrete members exhibit attractive structural advantages over their bare steel or reinforced concrete counterparts. Through the appropriate use of the mechanical properties of the two materials, a steel/concrete composite member can achieve comparatively favourable performance. In addition, the use of partially-encased profiles (where concrete is cast between the flanges of a steel I or H section) offers a number of practical benefits in terms of the omission of formwork and the possibility of using conventional steel connections to the flanges. This favourable performance and practical merits have led to an increased utilisation of partially-encased steel sections in seismic prone regions, particularly in Europe, and have prompted several investigations on the structural response of this form of member. (Elghazouli and Elnashai, 1993; Plumier et al., 1994; Broderick and Elnashai, 1994; Elghazouli and Treadway, 2008). However, it has also been recognised that the onset of flange local buckling can lead to reductions in moment capacities which, as is the case of partially-encased members, can be aggravated by the presence of axial loads. This limiting factor has motivated the use of alternative detailing, such as transverse links as a means for delaying the occurrence of flange buckling and the associated strength degradation.

This paper presents the results of a series of tests on Partially-encased composite members subjected to cyclic loading. The experimental study reported in this paper focuses on the inelastic performance of partially-encased members which incorporate buckling-delaying transverse links with different levels of co-existing axial loads. The experimental cyclic response of a partially-encased specimen detailed according to conventional European practice is also presented as the basis for comparison. A total of seven specimens with UC 152x23 sections, tested under major axis bending, are described. The testing arrangement and details of the specimens are presented, and the main results and observations are summarised. Finally, response parameters related to capacity and ductility, including energy dissipation and cumulative displacement at failure, are discussed.

2. EXPERIMENTAL DETAILS

2.1. Testing Arrangement

The self-reacting test-rig shown in Fig. 1 was used for the experimental programme. The experimental set-up was designed to apply lateral displacement on the tip of a vertical cantilever member while at the same time imposing constant axial loads at the top of the specimen (Ban, 2011). Fig. 1 also presents the dimensions of the set-up employed. The specimens were welded to a bottom plate of size 350x350x30 mm which in turn was bolted to a 500x500x50 mm plate attached to the self-reacting frame in order to ensure a rigid base support.

Displacements were applied at the top of the specimen using a double-acting actuator operating in displacement control. The actuator had a static capacity of ± 250 kN and a maximum stroke of ± 125 mm. The back of the actuator was stressed to a plate of dimensions 500x500x75 mm firmly connected to the reaction rig. Similarly, axial loads were applied through a vertical actuator of 500 kN capacity connected by means of low-friction swivel joints to the reacting frame as depicted in Fig. 1.

Lateral displacements and corresponding forces were recorded by the load cell and displacement transducer incorporated within the horizontal actuator. Likewise, the forces applied by the vertical actuator were recorded by means of a load cell attached to it. The out-of plane deformation of the specimen was monitored through a attached inclinometer while another inclinometer was placed in the member to confirm the angle of rotation. Displacement transducers placed along the height of the specimen were also used to measure member deformations. Strain gauges were used to monitor the strains at specific locations within the specimen. The cyclic testing protocol shown in Fig. 2 was used based on the recommendations provided by ECCS (1986), where Δ_y is the estimated yield displacement. After the maximum displacement was reached, all the specimens were subjected to additional displacement reversals at amplitudes of $\pm 5\Delta_y$ up to the occurrence of fatigue fracture.

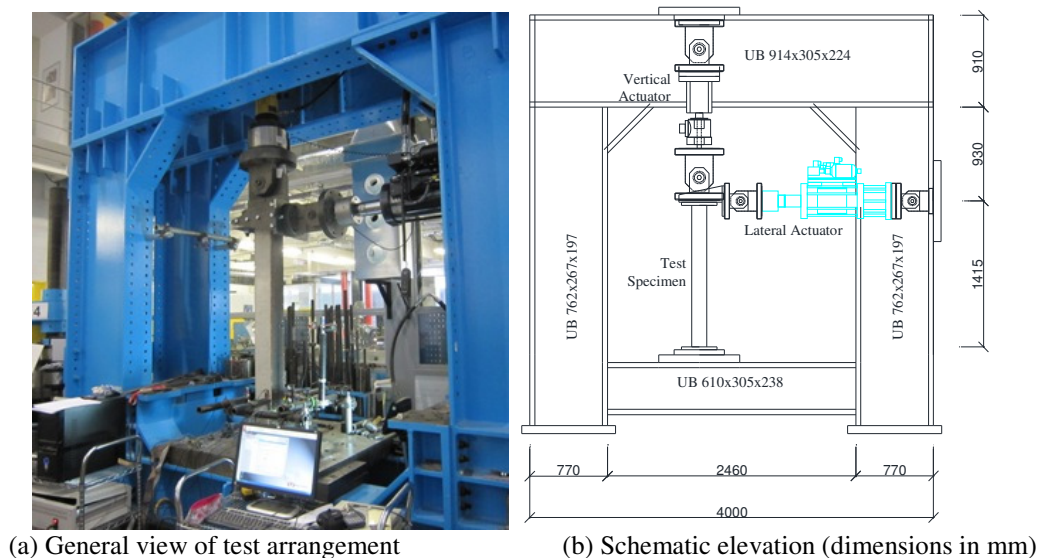


Figure 1. Experimental set-up

2.2. Specimens and materials

In total, seven partially-encased beam-column members were tested. A summary of the test series is given in Table 2.1. Note that UC refers to Universal Column. The constant axial load applied in each test is also given in the Table 2.1. Fig. 3 illustrates the three section configurations utilised. D8 stirrups spaced at 40 mm intervals were employed throughout the height of all specimens. Additionally, buckling-delaying links in the form of bars (Section Type B in Fig.3c) or plates (Section Type C in Fig. 3d) were employed over the plastic zone along 480 mm at the bottom of Specimens PE2 - PE7.

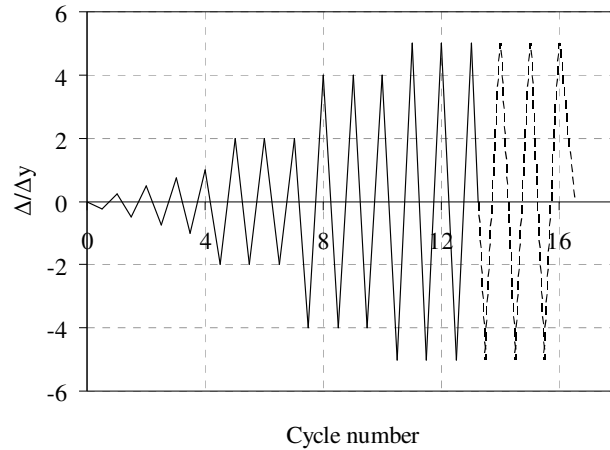
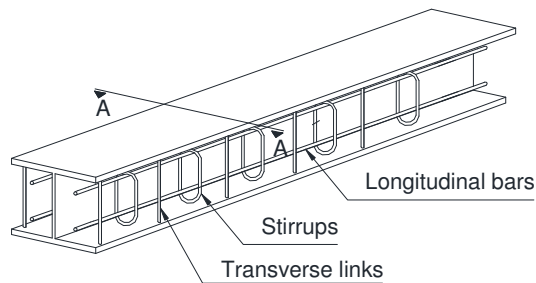


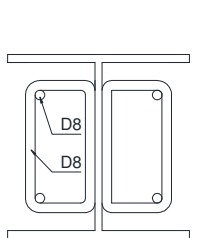
Figure 2. Cyclic testing protocol

Table 2.1. Summary of test programme

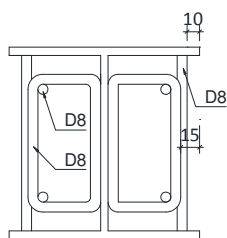
Specimen	Section	Axial load (kN)	Transverse links	Section Configuration (Fig. 3)
PE1	UC 152x23	125	None	A
PE2	UC 152x23	125	8@60	B
PE3	UC 152x23	125	12@40	B
PE4	UC 152x23	125	8@60	C
PE5	UC 152x23	125	12@40	C
PE6	UC 152x23	250	8@60	C
PE7	UC 152x23	250	12@40	C



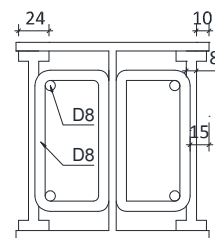
(a) Specimen view



(b) Section Type A



(c) Section Type B



(d) Section Type C

Figure 3. Details of section configurations (dimensions in mm)

The detailing of Specimens PE2 and PE3 included 8 mm steel bars running through purpose-drilled holes on the flange outstands and welded from the outside of the specimen, as depicted in Fig. 4. This additional detailing was provided in order to delay the onset of outward buckling of the steel flanges while at the same time avoiding the premature failure of the links caused by welding difficulties

(Elghazouli and Treadway, 2008). Nevertheless, as discussed below, the stress concentration in the area around the hole induced fracture of the steel flanges. Therefore, Specimens PE3 - PE7 were re-designed to incorporate an improved detail consisting of 8 mm thick I-shaped steel plates welded to the flange outstands on the inside as depicted in Fig. 5.



Figure 4. Specimen with additional buckling-delaying bars



Figure 5. Specimen with additional buckling-delaying plates

The average yield and ultimate stress, σ_y and σ_u , respectively, obtained from at least three samples taken from the flanges and webs of the steel members as well as the steel links are shown in Table 2.2. No formwork was needed for casting, and the two sides were cast three days apart. The average concrete cube strength at the time of testing is presented in Table 2.3.

Table 2.2. Material properties for steel components

Specimen	Plate	σ_y (MPa)	σ_u (MPa)
PE1	Section flange	458	575
	Section web	448	576
PE2	Section flange	458	575
	Section web	448	576
PE3	Transverse link	335	464
	Section flange	458	575
	Section web	448	576
PE4	Transverse link	335	464
	Section flange	401	558
	Section web	411	556
PE5	Transverse link	500	668
	Section flange	401	558
	Section web	411	556
PE6	Transverse link	500	668
	Section flange	401	558
	Section web	411	556
PE7	Transverse link	500	668
	Section flange	401	558
	Section web	411	556

Table 2.3. Concrete strength at time of testing

Specimen	Concrete Strength (MPa)
PE1	44
PE2	43
PE3	50
PE4	46
PE5	41
PE6	42
PE7	40

3. RESULTS AND OBSERVATIONS

The cyclic response of Specimens PE1 - PE7 is presented in Fig. 6 while the main response parameters are summarised in Table 3.1. It is clear from this figure and table that all specimens exhibited stable hysteretic behaviour with similar rates of energy dissipation. Flange buckling was followed by an immediate release of concrete confinement and gradual strength deterioration in all cases. In subsequent sub-sections, the experimental results and observations are discussed with particular focus on failure mechanisms and overall ductility considerations.

Table 3.1. Yield capacity of specimens

Specimen	Yield moment (kNm)	Lateral displacement at yield (mm)	Average rate of energy dissipation
PE1	74.5	25	64.6
PE2	77.0	22	64.9
PE3	76.3	25	61.9
PE4	74.7	24	64.6
PE5	78.6	23	64.0
PE6	66.7	22	63.2
PE7	63.0	23	61.8

3.1. Failure mechanisms

Specimen PE1, which presents a conventional European detail, experienced local buckling at the first $4\Delta_y$ excursion. The half wavelength of the flange buckles was approximately 140 mm. Fig. 7 shows the extent of local buckling as well as spalling of the concrete cover accompanied by buckling of the longitudinal reinforcement.

The effectiveness of the welded bars in delaying local buckling was clearly observed in Specimens PE2 and PE3. Nevertheless, fracture initiated in the holes drilled to accommodate the bars and propagated over the both flanges as illustrated in Fig. 8. This premature fracture prevented any significant enhancement in the ductility of these specimens in comparison with Specimen PE1.

In order to avoid the complications associated with outside welding of the buckling-delay links, Specimens PE4 - PE7 incorporated I-shaped steel plates welded on the inside. Fig. 9 presents the failure mechanism observed in Specimen PE4 (with links spaced at 60 mm intervals). It can be observed from this figure that the half wavelength of the flange buckles was determined by the link spacing in this case. It can also be noted from Fig. 9, that the large strains developed in the buckled area lead to low-cycle fatigue fracture in the flange and links. However, as discussed below, it should be noted that this only took place after significant levels of cumulative deformation. A similar failure mechanism was observed for Specimen PE6 in which the axial load was doubled while retaining all other geometric characteristics.

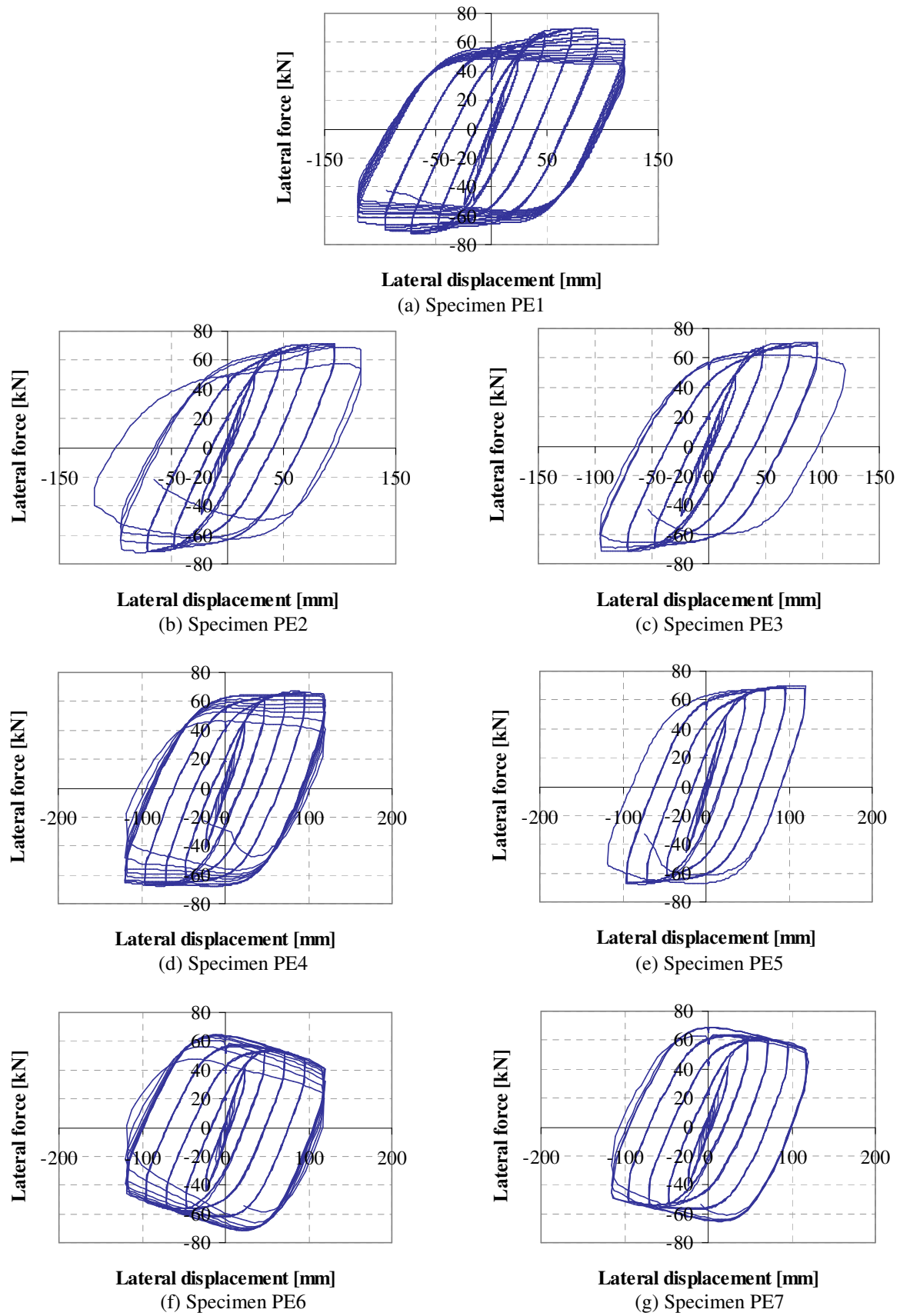


Figure 6. Cyclic load-displacement response



Figure 7. View of Specimen PE1 after testing



Figure 8. Low-cycle fatigue fracture in Specimens PE2 (left) and PE3 (right)



Figure 9. Low cycle fatigue fracture in Specimen PE4: link fracture (left) flange-through fracture (right)

In the case of Specimens PE5 and PE7 where the spacing of the additional I-shaped links was reduced to 40 mm, low-cycle fatigue fracture took place at the fixed end of the specimens within the heat affected area near the welding zone between the member and the rigid plate at the bottom. No significant buckling of the flanges was observed before the occurrence of fracture as depicted in Fig. 10 for Specimen PE7. A similar failure mechanism was observed for Specimen PE5.



Figure 10. Low cycle fatigue fracture in Specimen PE7

3.2. Energy dissipation

Fig. 11 presents an assessment of the energy dissipation of the tests described above. The curves depict the cumulative dissipated energy versus cumulative rotation, while the rates of energy dissipated per unit rotation is given in Table 3.1. Fig. 11 also shows the cumulative rotations at failure represented by vertical dashed lines. Importantly, failure is defined as the occurrence of fatigue fracture in any component of the specimen or the attainment of a 20% reduction in capacity; whichever occurs first. A summary of the energy dissipation parameters at ultimate is presented in Table 3.2.

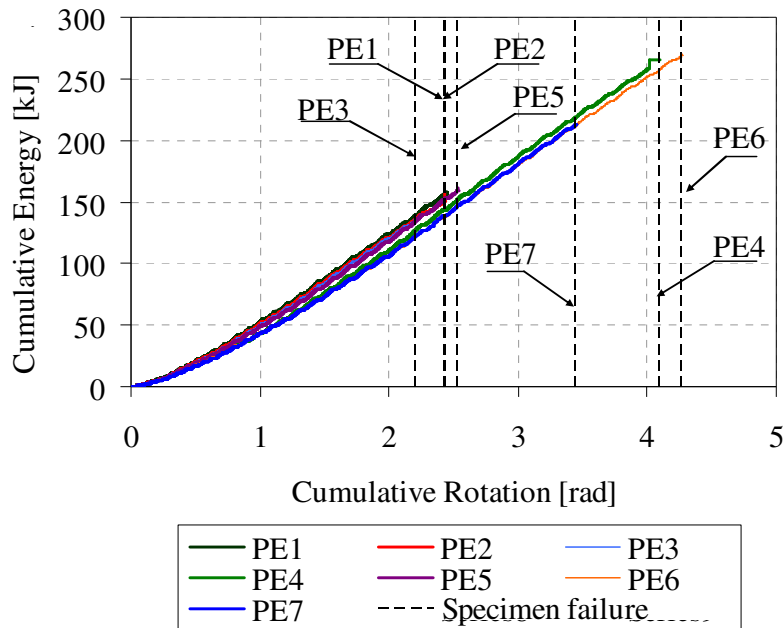


Figure 11. Cumulative energy dissipation

Table 3.2. Energy dissipation parameters

Specimen	Total dissipated energy (kJ)	Cumulative rotation at failure (rad)
PE1	157.6	2.44
PE2	157.7	2.43
PE3	136.2	2.20
PE4	264.9	4.10
PE5	161.8	2.53
PE6	270.0	4.27
PE7	213.3	3.45

It can be observed from Fig. 11 and Table 3.2 that despite the similar energy dissipation rates of all specimens examined, there is a substantial enhancement in the total energy dissipation capabilities of members incorporating improved buckling-delaying links (e.g. Specimens PE4 - PE7) when compared with the conventional partially-encased detail (i.e. Specimen PE1). The provision of I-shaped steel links results in a 70% increase in the total dissipated energy and associated enhancements in the cumulative rotation at failure when an axial load of 10% of the axial capacity of the member is present (Specimen PE4 versus PE1). Furthermore, an increase in the level of axial load (up to 20% of the axial capacity in Specimen PE6) does not affect the energy dissipation capacity of the improved detail, with Specimen PE6 able to withstand 75% more cumulative displacement than its conventional counterpart (Specimen PE1) while simultaneously sustaining double the axial action.

7. CONCLUSION

The experimental inelastic behaviour of partially-encased composite steel/concrete members was examined in this paper. The test set-up, specimen configuration and material properties were outlined, and the results of seven tests were summarised. The tests were carried out under cyclic conditions representing severe seismic loading, with varying levels of axial loads representing gravity conditions. The test results provide essential data for the validation and calibration of analytical and design studies. The experimental findings also enable a direct assessment of the influence of improved buckling-delaying details on the energy dissipation and failure mechanism of this type of composite member.

The effectiveness of buckling-delaying links was demonstrated and the response of two link configurations was compared. Specimens incorporating welded bars failed by fracture in the flanges instigated by the provision of holes drilled to accommodate the additional bars. Subsequently, fracture propagated over both flanges preventing a significant enhancement in the ductility of these specimens.

In order to avoid the complications associated with outside welding of the buckling-delaying links, a new detail incorporating I-shaped steel plates welded on the inside was proposed. It was shown that this improved detail was able to increase the total energy dissipation and the corresponding cumulative deformation capacity of partially-encased members by about 70% when compared with conventional details.

REFERENCES

- Ban, X. (2011). Inelastic performance of composite steel/concrete members. Master of Philosophy report, Imperial College London
- Broderick, B.M. and Elnashai, A.S. (1994). Seismic resistance of composite beam-columns in multi-story structures. *Journal of Constructional Steel Research*, **30**, 231-258
- Chicoine, T., Tremblay, R., Massicotte, B., Ricles, J. and Lu, L.W. (2002) Behaviour and strength of partially encased composite columns with built-up shapes. *Journal of Structural Engineering ASCE*, **128:3**, 278-288.
- ECCS. European Convention for Constructional Steelwork (1986) Recommended testing procedure for assessing the behaviour of structural steel elements under cyclic loads, Brussels
- Elghazouli, A.Y. and Elnashai, A.S. (1993) Performance of composite steel/concrete members under earthquake loading. *Earthquake Engineering and Structural Dynamics*, **22**, 347-368
- Elghazouli, A.Y. and Treadway, J. (2008) Inelastic behaviour of composite members under combined bedding and axial loading. *Journal of Constructional Steel Research*, **64**, 1008-1019
- Plumier, A., Abed, A., and Tilioune, B. (1994) Increase of buckling resistance and ductility of Hsections by encased concrete. *Behaviour of steel structures in seismic areas: STESSA'94*, F. M. Mazzolani and V. Gioncu, eds., E & FN Spon, 211-220
- Schleich, J.B. (1988) Fire engineering design of steel structures. *Steel construction today*, **2**, 39-52

